Experimental and Computer Modeling Studies of Micellar Diastereoselectivity

Robert A. Moss,* Thomas F. Hendrickson, Ryuichi Ueoka,*[1] Kwang Yoo Kim, and Paul K. Weiner*

Contribution from the Department of Chemistry, Rutgers, The State University of New Jersey, New Brunswick, New Jersey 08903. *Received September 19, 1986*

Abstract: Diastereomeric dipeptide *p*-nitrophenyl esters, Z-(D or L)-Pro-L-Pro-PNP or Z-(D or L)-Trp-(L)-Pro-PNP, were cleaved at pH 8 in buffer, nonfunctional cetyltrimethylammonium (CTA) ion micelles, and in thiolate- or iodosobenzoate-functionalized micelles. Kinetic diastereoselectivities were measured. In buffer or CTA micelles, intermolecular hydroxide ion cleavage of Z-Pro-Pro-PNP is LL diastereoselective and pH independent ($k^{LL}/k^{DL} \sim 2$ from pH 8.0–10.7). Similar cleavage of Z-Trp-Pro-PNP is DL diastereoselective at pH 8.0 ($k^{LL}/k^{DL} = 0.3$), due to base-activated intramolecular diketopiperazine cyclization, but LL diastereoselective at higher pH ($k^{LL}/k^{DL} = 2.0$ in CTA micelles, pH 10), where the attack of hydroxide ion at the ester carbonyl is dominant. In functional micelles, both substrates show markedly enhanced, LL diastereoselectivity at pH 8, attending nucleophilic carbonyl attack by the micellar thiolate or iodosobenzoate functional groups. Combinations of molecular mechanics and molecular orbital calculations, as well as computer graphics methods, were used to determine preferred conformations and energies for the ground-state Pro-Pro diastereomeric substrates and for the tetrahedral intermediates derived from them upon carbonyl attack by hydroxide ion or a surfactant cholinate nucleophile. An analysis of the differential energies between tetrahedral intermediates and their corresponding ground-state conformers reproduces the sense of the kinetic diastereoselectivities. The origins of the selectivity and its amplification by functional micelles are discussed.

Exploring the stereochemical component of the "micelle-enzyme analogy",[2] we have examined the kinetic diastereoselectivity attending cleavages of the dipeptide esters of structures Z-(L)-AA-(L)-Pro-PNP or Z-(D)-AA-(L)-Pro-PNP, where AA = Ala, Phe, Trp, Leu, and Val, cleaved by a variety of nonfunctional [cetyltrimethylammonium (CTA)] and functional (particularly long chain thiocholine) aqueous micellar surfactants.[3,4] These kinetic selectivity studies were extended to the Z-(D or L)-Phe-(D or L)-Phe-(L)-Pro-PNP tripeptide diastereomeric substrates[5] and to vesicular[6] or coaggregate[7] (mixed single/double chain surfactant) cleavages of various dipeptide, tripeptide, and (enantiomeric) amino acid esters.

We found that nucleophile-functionalized micellar or vesicular surfactants invariably cleaved the di- or tripeptide ester substrates with the L configuration at the amino acid adjacent to the C-terminal proline faster than they cleaved the diastereomeric substrates with a D adjacent amino acid.[3,5,6,7] A molecular-level rationalization for the LL diastereoselectivity was derived from the inspection of hand-held CPK molecular models, based on the apparent 1:1 interactions between the various conformers of substrate diastereomers and a represenstative long chain thiocholinate surfactant reagent, $RN^+Me_2CH_2CH_2S^-$.[8]

More recently, we discovered that the LL diastereoselectivity observed in the thiocholine surfactant cleavage of the Z-(D or L)-Trp-(L)-Pro-PNP substrates did not arise solely from 1:1 surfactant/substrate interactions. Indeed, reactions in the "small" micelles formed at concentrations just above the surfactant's critical micelle concentration (cmc) were *not* diastereoselective. The onset of selectivity was associated with a second "critical" surfactant concentration that lay ~5 times above the classical cmc.[9] Clearly, the diastereoselectivity originated in supramolecular interactions of the substrate and the micellar assembly.

Just as clearly, a more sophisticated modeling treatment is required for these reactions. As an initial step on this road, we undertook a combined experimental/computer modeling study of the micellar cleavage of the Z-(D or L)-Pro-(L)-Pro-PNP diastereomers. The Pro-Pro substrates were chosen to minimize the number of substrate conformations that we would have to consider in the modeling studies.

Molecular mechanics methods are coming into general use as a tool for the examination of conformation and reactivity.[10] Recently, a combination of ab initio quantum mechanical and molecular mechanics methods was used to study the cleavage of formamide by hydroxide ion in the gas phase and in aqueous solution; good agreement was found between calculated and experimental reaction and activation energies.[11] Molecular mechanics has also been used to refine protein structures and to model the binding of substrates to enzymes.[12]

To identify the low-energy conformations of our Z-Pro-Pro-PNP substrates, we chose the AMBER molecular modeling package,[13] together with several computer graphics programs. We also used the MNDO semiempirical molecular orbital method[14] to generate a model tetrahedral intermediate for a simple esterolysis reaction and then used the resulting reaction center geometry in molecular mechanics modeling of tetrahedral intermediates for the esterolysis of the Z-Pro-Pro-PNP substrates.

Although the LL/DL diastereoselectivities that we encounter experimentally are relatively small, and represent differential activation energies <2 kcal/mol, the calculational results are in overall agreement with the empirical findings. Of course we make no claim for exclusivity or establishment of our model on this basis. Indeed, given the complexity of the reactant system, the uncertainties of micellar structure, and the arbitrary nature of our procedure, we hold a modest assessment of the results. Nevertheless, the present combined empirical and computational approach to the problem of micellar stereoselectivity is, so far as we know, the first of its kind and represents a beginning that we

(1) Visiting Professor on leave from the Department of Industrial Chemistry, Faculty of Engineering, Kumamoto Institute of Technology, Ikeda, Kumamoto 860, Japan.

(2) Fendler, J. H.; Fendler, E. J. *Catalysis in Micellar and Macromolecular Systems*; Academic Press: New York, 1975; pp 100–102.

(3) (a) Moss, R. A.; Lee, Y. S.; Lukas, T. J. *J. Am. Chem. Soc.* **1979**, *101*, 2499. (b) Moss, R. A.; Lee, Y. S.; Alwis, K. W. *Ibid.* **1980**, *102*, 6646.

(4) Moss, R. A.; Lee, Y.-S. *Tetrahedron Lett.* **1981**, *22*, 2353.

(5) Moss, R. A.; Lee, Y.-S.; Alwis, K. W. *Tetrahedron Lett.* **1981**, *22*, 283.

(6) Moss, R. A.; Taguchi, T.; Bizzigotti, G. O. *Tetrahedron Lett.* **1982**, *23*, 1985.

(7) Ueoka, R.; Matsumoto, Y.; Yoshino, T.; Hirose, T.; Moss, R. A.; Kim, K. Y.; Swarup, S. *Tetrahedron Lett.* **1986**, *27*, 1183.

(8) Review: Moss, R. A.; Lee, Y.-S. In Green, B. S.; Ashani, Y.; Chipman, D. *Studies in Organic Chemistry*; Elsevier: Amsterdam, 1982; Vol. 10, pp 200–218. This review contains photographs of molecular models of the substrates and presumed activated complexes.

(9) (a) Moss, R. A.; Chiang, Y.-C.P. *Tetrahedron Lett.* **1983**, *24*, 2615. (b) Moss, R. A.; Chiang, Y.-C.P.; Hui, Y. *J. Am. Chem. Soc.* **1984**, *106*, 7506.

(10) Burkert, U.; Allinger, N. A. *Molecular Mechanics*; American Chemical Society: Washington, DC, 1982; Monogr. No. 177.

(11) Weiner, S. J.; Singh, U. C.; Kollman, P. A. *J. Am. Chem. Soc.* **1985**, *107*, 2219.

(12) Wipff, G.; Dearing, A.; Weiner, P. K.; Blaney, J. M.; Kollman, P. A. *J. Am. Chem. Soc.* **1983**, *105*, 997. Naruto, S.; Motoc, I.; Marshall, G. R.; Daniels, S. B.; Sofia, M. J.; Katzenellenbogen, J. A. *Ibid.* **1985**, *107*, 5262.

(13) Weiner, P. K.; Kollman, P. A. *J. Comput. Chem.* **1981**, *2*, 287.

(14) Dewar, M. J. S.; Thiel, W. *J. Am. Chem. Soc.* **1977**, *99*, 4899, 4907.

0002-7863/87/1509-4363$01.50/0

Table I. Diastereoselectivity in the Buffer or Micellar CTACl Cleavages of Diastereomeric Dipeptide Esters[a]

		Z-Trp-Pro-PNP[b]			Z-Pro-Pro-PNP[b]		
pH	medium	$10^3k_\psi^{LL}$	$10^3k_\psi^{DL}$	k_ψ^{LL}/k_ψ^{DL}	$10^3k_\psi^{LL}$	$10^3k_\psi^{DL}$	k_ψ^{LL}/k_ψ^{DL}
8.0	buffer[c]	0.09	0.31	0.30	0.097	0.053	1.8
8.0	CTACl[c]	1.17	4.12	0.28			
9.0	buffer				1.02	0.51	2.0
9.0	CTACl	5.91	9.72	0.61			
9.3	CTACl	9.62	11.9	0.81			
9.6	CTACl	18.8	11.8	1.6			
9.6	buffer	0.17	0.12	1.4			
10.0	CTACl	28.1	13.9	2.0	7.06	3.51	2.0
10.7	CTACl	116	37.8	3.1	38.6	16.5	2.3
10.7	buffer				5.51	3.45	1.6

[a] Conditions: [CTACl] = 5×10^{-3} M, [substrate] = 2×10^{-5} M, 25 °C. Buffers: pH 8–10.0, 0.02 M Tris in 0.05 M aqueous KCl; pH 10.7, 0.02 M borax in 0.05 M aqueous KCl. [b] Rate constants are in s^{-1}. See text for a discussion of kinetic methods. Reproducibilities of the rate constants were about ±3% in duplicate runs. [c] These data are from ref 3b, in 0.02 M phosphate buffer, μ = 0.05 (KCl).

hope will be followed by increasingly sophisticated and accurate reaction simulations.

Results and Discussion: Experimental Studies

Surfactants and Substrates. The three surfactants we used extensively are cetyltrimethylammonium chloride (CTACl, **1**), thiocholine surfactant **2** (16-SH), and the iodosobenzoate derivative **3** (16-IO). CTACl is commercially available, whereas the

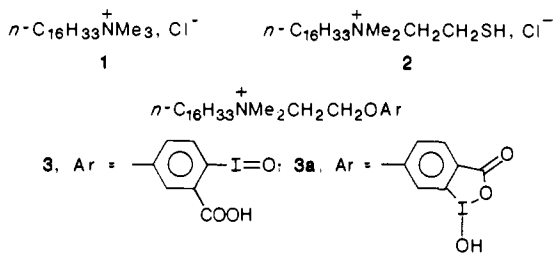

synthesis and properties of 16-SH[15] and 16-IO[16] have been described. The *o*-iodosobenzoate group of 16-IO largely exists not in the classical form expressed by **3** but in the valence tautomeric 1-hydroxy-1,2-benziodoxolin-3-one form (**3a**).[16] Under the kinetic conditions we employ, where pH ~8, both micellar 16-SH (pK_a ~ 7.3[15]) and 16-IO (pK_a ~ 6.5[16]) are extensively ionized to their zwitterionic S^- or O^- forms.

The principal substrates used in this study are the diastereomeric dipeptide *p*-nitrophenyl (PNP) esters of carbobenzyloxy Z-(D or L)-prolyl-(L)-proline: DL- or LL-**4** (Z-Pro-Pro-PNP). These di-

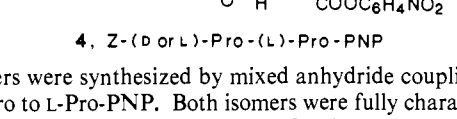

4, Z-(D or L)-Pro-(L)-Pro-PNP

astereomers were synthesized by mixed anhydride coupling of (D or L)-Z-Pro to L-Pro-PNP. Both isomers were fully characterized, and details appear in the Experimental Section. For comparison, we also made some kinetic studies on the Z-(D or L)-Trp-(L)-Pro-PNP substrates, **5**. These were available from a previous investigation and have been fully described.[9b]

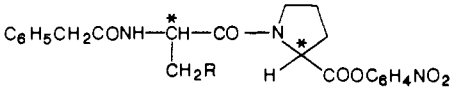

5, Z-(D or L)-Trp-(L)-Pro-PNP (R = 3-indolyl)

Kinetic Studies (Methods). Pseudo-first-order rate constants (k_ψ) for cleavage of the dipeptide esters were evaluated by spectroscopically monitoring the release of *p*-nitrophenoxide ion at 400 nm. Rapid reactions (k_ψ > 0.01 s^{-1}) were followed by stopped-flow methods, whereas slower reactions (k_ψ < 0.01 s^{-1}) were monitored with a conventional spectrophotometer. Stopped-flow reactions (with **5**) were initiated by rapid mixing of a double strength buffer solution with an aqueous solution of **5** and surfactant adjusted to pH 4 with HCl or (with **4**) by rapid mixing of a buffer solution of substrate with a buffer solution of surfactant. Slower reactions were initiated by addition of a dioxane stock solution of substrate (final [dioxane] = 0.1 vol·%) to buffer/surfactant or buffer solutions. Buffers included 0.02 M aqueous phosphate, Tris, or borax, with μ = 0.02 or 0.05.

Buffer or CTACl Hydrolysis. The Trp-Pro and Pro-Pro substrates were hydrolyzed in buffer and in micellar CTACl/buffer solutions at various pHs; k_ψ for the release of $PNPO^-$ was obtained for DL and LL isomers. These results are recorded in Table I, together with the kinetic diastereoselectivity, k_ψ^{LL}/k_ψ^{DL}, for each reaction. Inspection of the results affords the following observations: (a) With either substrate set and for either diastereomer within each set, k_ψ increases with increasing pH. (b) Cleavage reactions in micellar CTACl are faster than the comparable reactions in buffer alone at any given pH, but k_ψ^{LL} and k_ψ^{DL} are enhanced comparably, so that their ratio, the diastereoselectivity, is similar in micellar or buffer solutions. (c) Cleavage of the Z-Trp-Pro-PNP isomers is DL diastereoselective at low pH (k_ψ^{LL}/k_ψ^{DL} ~ 0.3 at pH 8.0) but smoothly changes to LL diastereoselective as the pH increases (k_ψ^{LL}/k_ψ^{DL} ~ 3 at pH 10.7). (d) The cleavage of the Z-Pro-Pro-PNP diastereomers, on the other hand, is LL diastereoselective at pH 8 and effectively pH independent over the range 8.0–10.7.

Observations a and b are readily interpreted; esterolyses of these substrates are catalyzed by hydroxide ions, so that k_ψ increases with pH; substrate bound to micellar CTACl is cleaved more rapidly than substrate in bulk aqueous solution because the local $[OH^-]$ is elevated at the surface of cationic micelles.[17] Observations c and d are more intriguing, and their analysis requires a detailed examination of the available mechanisms for esterolysis. In particular, two paths exist for hydroxide mediated cleavages of Z-AA-Pro-PNP; cf. eq 1. Direct attack by OH^- can occur

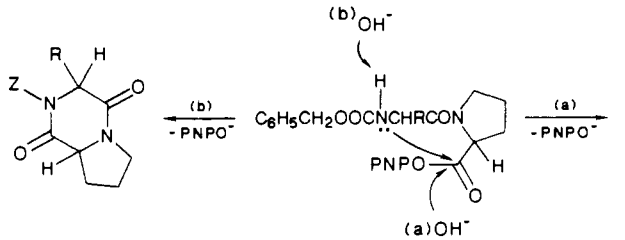

Z-AA-Pro(COOH) (1)

at the substrate's scissile carbonyl, leading to Z-AA-Pro(COOH), path a, or attack can occur at the N–H of the distal amino acid, activating nitrogen as an internal nucleophile and leading, via cyclization, to a diketopiperazine (DKP), path b.[18]

(15) Moss, R. A.; Bizzigotti, G. O.; Huang, C.-W. *J. Am. Chem. Soc.* **1980**, *102*, 754.
(16) Moss, R. A.; Kim, K. Y.; Swarup, S. *J. Am. Chem. Soc.* **1986**, *108*, 788.
(17) Cf.; Bunton, C. A. *Catal. Rev. Sci. Eng.* **1979**, *20*, 1.

Table II. Diastereoselectivity in the Functional Micellar Cleavages of Diastereomeric Dipeptide Esters, 25 °C

surfactant	Z-Trp-Pro-PNP[a]			Z-Pro-Pro-PNP[a]		
	k_ψ^{LL}	k_ψ^{DL}	k_ψ^{LL}/k_ψ^{DL}	k_ψ^{LL}	k_ψ^{DL}	k_ψ^{LL}/k_ψ^{DL}
none[b]	9×10^{-5}	31×10^{-5}	0.30	9.7×10^{-5}	5.3×10^{-5}	1.8
16-SH (**2**)[c]	24.4	4.85	5.0	7.27	1.26	5.8
16-IO (**3a**)[d]				0.810	0.107	7.6

[a] Pseudo-first-order rate constants in s^{-1}. Reproducibilities of duplicate runs were better than ±4% of the mean value. [b] Buffer alone at pH 8.0; see Table I. [c] [16-SH] = 4×10^{-3} M, [substrate] = 2×10^{-5} M, pH 7.8, 0.02 M phosphate buffer, 0.05 M KCl. [d] [16-IO] = 2×10^{-4} M comicellar in 2×10^{-3} M CTACl, [substrate] = 2×10^{-5} M, pH 8.2 in 0.02 M Tris buffer, 0.05 M KCl.

In fact, OH^--induced cleavages of the Z-Trp-Pro-PNP diastereomers predominantly follow path b at pH 8 in either CTACl or buffer solutions: the DKP products can be isolated in >70% yields from the reaction product solutions.[4] Moreover, the DKP/Z-Trp-Pro(COOH) product ratios from the DL and LL substrates quantitatively reflect the k_ψ^{LL}/k_ψ^{DL} kinetic ratios and the observed DL diastereoselectivity. Intramolecular cleavage to the DKP is kinetically favored with the DL (relative to the LL) isomer because DKP formation from the latter is sterically hindered by interactions between the syn-disposed R (CH_2-3-indolyl) and proline (CH_2)$_3$ moieties during cyclization.[4,19] Indeed, DL diastereoselectivity appears to be general for the pH 8 buffer or CTACl micellar hydrolyses of Z-AA-Pro-PNP substrates, where AA = Ala, Phe, Leu, and Val, in addition to Trp.[3b,4]

As the pH increases, however, the diastereoselectivity of the Z-Trp-Pro-PNP cleavages swings from DL to LL. We suggest that this reflects increasing participation of the *intermolecular* OH^-/carbonyl cleavage, path a of eq 1. In keeping with this proposal, note that cleavages of the Z-Pro-Pro-PNP diastereomers, which *lack* an activatable NH group on the distal AA and cannot traverse path b, exhibit only LL diastereoselectivity at *any* pH. The Pro-Pro results suggest that path a, carbonyl/OH^- cleavage, has an intrinsic pH-independent LL diastereoselectivity, with $k_\psi^{LL}/k_\psi^{DL} \sim 2$. A similar LL diastereoselectivity is observed for the Trp-Pro substrates at higher pH (~10), where the carbonyl/OH^- path dominates.[20]

The principal observation to recall for further discussion below is the LL diastereoselectivity associated with external nucleophilic attack on the scissle carbonyl groups of the Z-Pro-Pro-PNP diastereomers. We will want to see if this kinetic bias can be modeled by the calculational studies.

Esterolysis by Functional Surfactants. In contrast to the DL kinetic diastereoselectivity manifested by Z-AA-(L)-Pro-PNP substrates during pH 8 buffer or CTACl nonfunctional micellar cleavages, functional surfactant micelles elicit striking rate enhancements and pronounced LL diastereoselectivity.[3b,4] These observations hold for AA = Ala, Phe, Leu, and Val,[3b] as well as for Trp (cf., Table II). For the Z-Trp-Pro-PNP isomers, we know that the 15-fold DL to LL swing in diastereoselectivity is a consequence of mechanistic change as the sterically controlled, anchimerically assisted, DL-diastereoselective, intramolecular esterolyses that occur at pH 8 in buffer or nonfunctional micelles give way to intermolecular nucleophilic cleavage in functional micelles (e.g., 16-S^-, where the nucleophile is the alkyl thiolate[3b]).

The Z-Pro-Pro-PNP substrates exhibit related chemistry (Table II). Here, the absence of a suitable adjacent AA obviates intramolecular closure in pH 8 buffer or micellar CTACl, so that these esterolyses occur with a modest, pH-independent, hydroxide-catalyzed LL diastereoselectivity. However, functional micellar cleavage with 16-SH/16-S^- brings about enormous [24 000 (DL) to 75 000 (LL)] rate enhancement and a threefold larger LL diastereoselectivity. With the comicellar iodosobenzoate/CTACl surfactant system, rate enhancements are reduced 10-fold, but the LL diastereoselectivity rises to 7.6, four times greater than in buffer alone.[21]

We offered a rationalization for the LL diastereoselectivity developed in cleavages of Z-AA-(L)-Pro-PNP substrates by functional surfactants such as 16-SH.[3b,8] Key elements included the following: (a) substrates react from "extended" (trans) conformations; (b) activated complexes are derived from 1:1 approximation of 16-S^- and the DL or LL substrate molecules; and (c) the hydrophobic "fit" of the 16-S^- methylene chain is better with the LL substrate and optimally positions the surfactant's thiolate for attack on the scissile carbonyl group.

Our recent work on the origins of micellar diastereoselectivity[9] suggests that this set of postulates is inadequate. The 1:1 surfactant/substrate activated complex does not account for the large rate enhancements that occur *without* stereoselectivity and are observed in the concentration regime cmc < [surfactant] < 5 cmc. The finding that a *second* type of micelle, formed at surfactant concentrations >5 cmc, is needed to evoke diastereoselectivity suggests that stereoselection is probably a cooperative effect involving substrate and at least several neighboring surfactant molecules.

Now, using computer modeling rather than the previously employed inspection of hand-held models, we seek more precise descriptions of reactive substrate conformers, 1:1 substrate/surfactant complexes, transition states, and 2:1 surfactant/substrate assemblies. In the last case, we take a step toward modeling stereoselective micellar reactions.

Procedures for Calculational Studies

Methods. Energy calculations were performed with the AMBER[13] molecular mechanics software package implemented on a VAX-11/780 computer. The force field and parameters have been fully documented elsewhere.[22] Additional required parameters that were not in the AMBER parameter set have been included in the supplementary material. The empirical energy function for the system is composed of terms that represent bond stretching, bending, and torsions, as well as nonbonded (van der Waals and electrostatic) terms, eq 2. The energy is refined by

$$E_{total} = \sum_{bonds} k_r(x_0 - x)^2 + \sum_{angles} k_\theta(\theta_0 - \theta)^2 + \sum_{dihedrals} \frac{k}{2}(1 + \cos(n\phi - \gamma)) + \sum_{i<j} \left(\frac{B_{ij}}{R_{ij}^{12}} - \frac{A_{ij}}{R_{ij}^{6}} + \frac{q_i q_j}{\epsilon R_{ij}} \right) \quad (2)$$

using minimization with analytical gradients until the root-mean-square gradient of the energy is less than 0.1 kcal/Å.

Residues. Residues not in the AMBER data base were created by using standard bond lengths and angles. MNDO[14] was then used to calculate atomic charges. We used the united atom force field of AMBER, so that any hydrogen charges in CH, CH_2, and CH_3 groups were added to the carbon atom to which they were bonded, and then the hydrogen atoms were removed from the coordinate set. The D-proline residue was assigned the same nuclear charges as L-proline. All newly created residues and their

(18) The DKP mechanism was described by Goodman and Stueben (Goodman, M.; Stueben, K. C. *J. Am. Chem. Soc.* **1962**, *84*, 1279) for (*Z*)-Gly-Pro-PNP, but diastereoselectivity was not relevant because of the achiral Gly.

(19) Cyclization from DL-**5** places these substituents in the more favorable anti arrangement. Cf.: ref 4. Bodanszky, M. In *The Peptides*; Gross, E., Meienhofer, J., Eds.; Academic Press: New York, 1979; Vol. 1, pp 161–162.

(20) The DKP products are not stable at high pH due to hydrolysis to the open Z-Trp-Pro(COO^-) product,[4] so that quantitation of DKP formation is impractical at pH 10.

(21) The LL diastereoselectivity is further enhanced at pH 8.2 in *vesicular* 16-IO/(n-$C_{16}H_{33})_2N^+Me_2,Cl^-$, where $k_\psi^{LL} = 0.73\ s^{-1}$, $k_\psi^{DL} = 0.075\ s^{-1}$, and $k_\psi^{LL}/k_\psi^{DL} = 9.7$. By lowering the reaction temperature to 20 °C, the diastereoselectivity can be increased to 13.2 (Ueoka, R.; Moss, R. A., unpublished observations).

(22) Weiner, S. J.; Kollman, P. A.; Case, D. A.; Singh, U. C.; Ghio, C.; Alagona, G.; Profeta, S., Jr.; Weiner, P. *J. Am. Chem. Soc.* **1984**, *106*, 765.

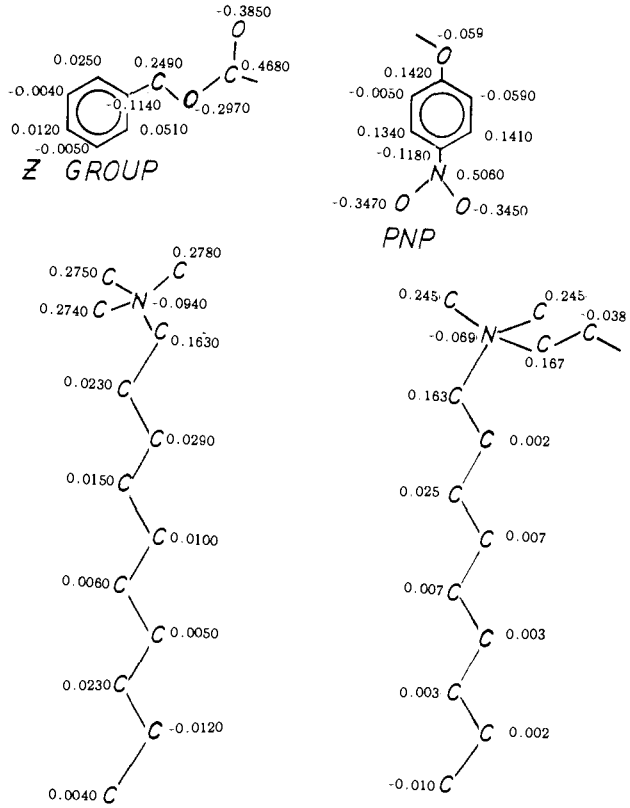

Figure 1. Residues created for molecular mechanics modeling studies. The numbers adjacent to each atom are the atomic charges derived from semiempirical MNDO[14] calculations.

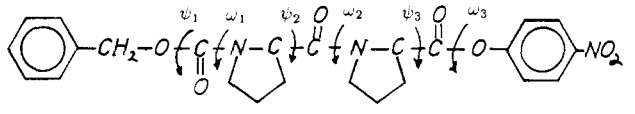

Figure 2. Z-Pro-Pro-PNP substrate molecule (**4**) showing the six dihedral angles that were varied in the conformational analysis. Although not strictly applicable, we have used the IUPAC–IUB rules for peptide backbones to define ψ_1 and ω_3, i.e., ψ_1 is defined as the angle C–O–C–N and ω_3 is defined as the angle C^{α}–C–O–C(Ar). All other dihedrals are defined in accordance with the IUPAC–IUB rules (see ref 37). For example, ψ_2 is defined as the angle N–C^{α}–C–N.

atomic charges are shown in Figure 1.

Starting Conformations. Initially, two conformers of both the DL and LL substrates (**4**) were manipulated with use of interactive graphics. These two conformers were either cis or trans at the peptide bond between the two proline rings. They were energy minimized with AMBER and then used to generate additonal conformations.

Inspection of the substrate molecule reveals that there are ten dihedral angles rotatable through 360°. Allowing for cis or trans "isomers" at the peptide bonds, and 30° rotations around the other bonds, the possible number of conformations is more than 10^9. In order to make the problem tractable, we decided to focus attention on those dihedrals associated with the amide and ester bonds. Graphical analysis showed that variations of these dihedrals caused the largest conformational changes in the substrate molecules. Furthermore, the dihedrals selected were those that had significant torsional barriers and were more likely to exhibit distinguishable conformational preferences.

We used a torsional mapping program[23] to calculate the relative energy changes associated with variations of two dihedrals at a time. Only the dihedral angles were allowed to vary, so that the rotational barrier height between any two conformations and the steepness of the walls are expected to be exaggerated. Six dihedral

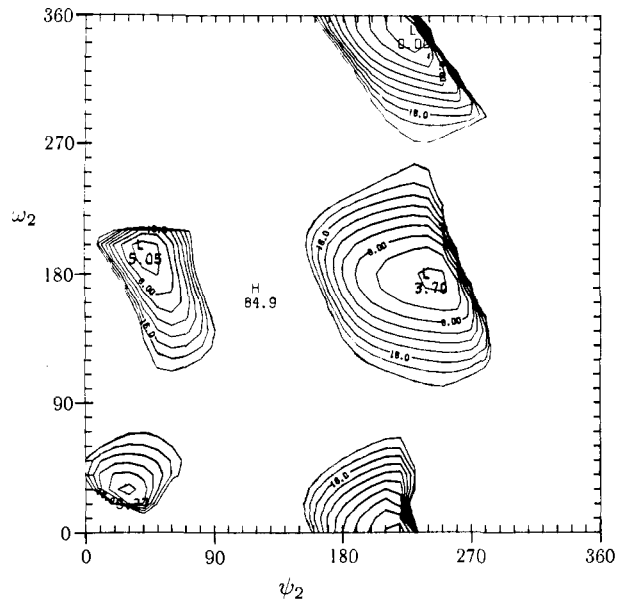

Figure 3. Torsional map illustrating the variations of the amide bond between the two proline rings (ω_2) and the dihedral between the α-carbon atom and the carbonyl carbon atom (ψ_2) (see also Figure 2). Energies were calculated at 10° increments of each angle, giving a 36 × 36 matrix of energy points. The contours illustrated here are for the LL diastereomer, starting with ω_2 at 0° (cis conformation). For this mapping, 3 minima are found besides the starting conformer, at 3.7, 5.05, and 9.27 kcal above the energy of the starting conformer. As a check, similar mapping was done starting from $\omega_2 \sim 180°$ (trans conformer). The contour interval is 2.0 kcal and the maximum contour mapped is 20 kcal above the minimum energy conformation.

angles were varied (labeled in Figure 2). From these torsional maps, a total of twenty possible conformational minima were found; eight for DL-**4** and twelve for the LL substrate. The LL diastereomer had more conformational minima because the dihedral angle corresponding to ψ_2 and ω_2 (Figure 2) had four minima for the LL isomer, whereas this angle had only two minima for the DL isomer. Although this did not constitute an exhaustive search of the conformational space, we feel it was representative of the major variations of the substrate molecules. A sample torsional map is illustrated in Figure 3.

Each of the resulting twenty conformations was then energy minimized at three values of dielectric (r, 3.0, and 30.0) in order to test the dependence of the calculated energies on the choice of dielectric. A complete tabulation of the conformational energies at each dielectric appears in the supplementary material. Using a distance dependent dielectric[24] (r) allows for short-range ion pairing and polarization effects, damps out long-range interactions, and is an implicit way of introducing solvent effects. The 1–4 electrostatic and nonbonded interactions were damped by a factor of 2 as recommended by Kollman.[22] With a few exceptions, the change in dielectric constant did not substantially change the energy ordering of the different conformations. However, when the larger dielectric constant (30) was used, the difference in energy between any two conformations became larger. Also, when the dielectric constant of 30 was used, the energy of any given conformation was 8–12 kcal higher than that of a similar conformation with use of a dielectric r. The energy difference between the lowest energy DL conformer and lowest energy LL conformer, using a dielectric r, was 1.76 kcal, with the DL diastereomer of lower energy. From the 20 conformations examined, the 3 lowest energy DL and 3 lowest energy LL conformers were selected for use in further analysis and calculation. Table III lists the energy contributions from bond strain, angle strain, etc., for these 6 conformers and defines pertinent nomenclature. Figure 2 defines the rotational angles that characterize the selected conformations,

(23) Gallion, S. L. Ph.D. thesis work, in progress at Rutgers University. The thank Mr. Gallion for the use of this program.

(24) Weiner, S. J.; Kollman, P. A.; Nguyen, D. T.; Case, D. A. *J. Comput. Chem.* **1986**, *7*, 230.

Table III. AMBER Energies for Ground-State Molecules[a]

energy (kcal/mol)	LC1	LC2	LT3	DT1	DT2	DT3
total	12.01	13.38	12.74	11.18	10.71	10.25
bond	0.55	0.51	0.51	0.54	0.53	0.50
angle	15.71	15.16	15.15	15.02	14.98	14.52
dihedral	13.26	14.91	13.93	14.14	14.69	14.46
VDW[b]	−13.53	−14.14	−9.77	−11.05	−13.57	−13.11
electric	−17.57	−16.80	−21.46	−22.53	−20.18	−20.44
1-4 VDW[c]	10.64	10.56	10.75	11.04	10.98	11.14
1-4 EEL[d]	2.96	3.18	3.63	4.01	3.28	3.17

[a] Calculations were performed with a distance dependent dielectric r. Nomenclature: LC1 refers to conformer "1" of LL-**4**, with a cis peptide bond; DT3 refers to conformer "3" of DL-**4**, with a trans peptide bond; and so on. In the cis Pro-Pro peptide bond both α-carbon atoms are cis with respect to a planar amide bond. [b] Lennard-Jones 6–12 interaction energy $(A/r^{12}) - (C/r^6)$ between atoms that are not mutually involved in a bond, a 1,3 bond angle, or a 1,4 dihedral angle. [c] The van der Waals interaction energy between the two terminal atoms of a dihedral angle that is between four connected atoms. [d] The electrostatic interaction energy $(q_i q_j/\epsilon r_{ij})$ between the two terminal atoms of a dihedral angle.

Table IV. Energy vs. Reaction Coordinate for Tetrahedral Intermediate **6**

energy (kcal/mol)	C–O distance (Å)[a]
−99.93	12.00
−104.62	3.00
−106.72	2.25
−137.28	1.70
−154.58	1.44

[a] Separation of the carbonyl carbon atom and the oxygen atom of the incoming hydroxide ion.

and Table VI lists the numerical values of these angles. Computer-generated drawings of the energy-optimized structures of (e.g.) conformers LC2 and DT2 can be found in Figure 5, A and B, respectively; see below.

Tetrahedral Intermediates. We modeled the esterolysis reactions of the DL and LL substrates in both bulk aqueous and micellar phases in an attempt to understand the origins of the observed diastereoselectivity. Our approach was as follows. First, we generated a tetrahedral geometry for the intermediate of a simple, model esterolysis reaction, using a MNDO semiempirical calculation.[14] As a model we chose the reaction of hydroxide ion with methyl acetate to form intermediate **6**; eq 3.

$$HO^- + CH_3COOCH_3 \longrightarrow CH_3-\underset{\displaystyle OH}{\overset{\displaystyle O^-}{\underset{|}{\overset{|}{C}}}}-OCH_3 \qquad (3)$$

6

The geometry determined for tetrahedral intermediate **6** was calculated by minimizing the energy with respect to all geometric variables, with no assumptions, using the Davidon–Fletcher–Powell (DFP) algorithm[25] as implemented in the MOPAC[26] calculation package.

We also performed calculations at several points along the coordinate of approach of the attacking hydroxide ion, the only constraint being a fixed C–OH distance. The distances chosen were 12.0, 3.00, 2.25, 1.70, and 1.44 Å, where 1.44 Å represents the *stationary point* for the tetrahedral intermediate found in the initial minimization. Table IV shows the energy as a function of the C–OH separation.

Results of these calculations are in qualitative agreement with previous calculations for tetrahedral intermediates in the gas phase.[11,27] We find that as the hydroxide ion approaches from 12.0 Å and the C–OH separation decreases to 1.44 Å the reaction is exothermic by 54.65 kcal/mol. The geometry of the intermediate, along with its atomic charges, is shown in Figure 4.

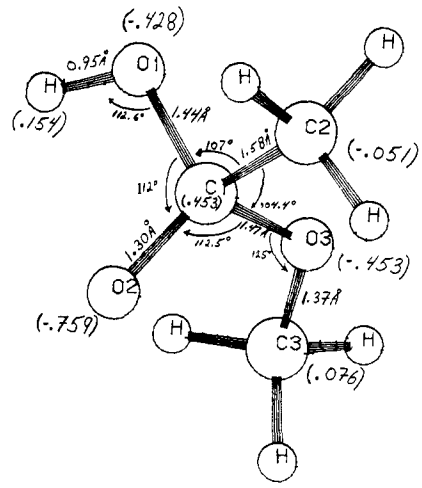

Figure 4. Tetrahedral intermediate **6** derived from the MNDO calculation. The numbers in parentheses are the atomic charges calculated from the electron density function for each atom. The pictured geometry about the carbonyl carbon was used in all subsequent molecular mechanics calculations of the tetrahedral intermediates corresponding to the substrate molecules.

Molecular Mechanics with the Tetrahedral Intermediate. Next, we took the tetrahedral geometry determined for **6** and inserted it into the lowest energy ground state conformations of **4** located above (cf. Table III). After insertion of the new geometries at the reaction centers, the systems were energy minimized with the new tetrahedral geometries as the only constraints, i.e., only those bond lengths and bond angles directly associated with sp^3-hybrid carbon were constrained. The difference in energy between a tetrahedral intermediate and its corresponding initial ground state was then taken as proportional to the activation energy of the reaction. In practice, a new residue was built which contained a covalent bond between the hydroxide oxygen and the peptide substrate. For all of the configurations studied, the starting geometry for minimization was obtained with use of interactive graphics.[28] The nucleophile was oriented approximately 2.0 Å away from the carbonyl carbon of the minimized ground-state substrate. This was the starting point for minimizing the tetrahedral intermediate. Although there are two faces of the reacting carbonyl group for possible nucleophilic attack, the conformers we worked with had one face sterically blocked by the rest of the substrate molecule. The OH^- was therefore permitted to approach the carbonyl carbon atom only from the unhindered face. This means that only one of the two possible configurations was generated at the new tetrahedral carbon of the resulting intermediate; i.e., only one diastereomer was permitted when the ground-state dipeptide ester was converted to the corresponding tetrahedral intermediate.

The values of the bond lengths and angles for the tetrahedral reaction center from the MNDO calculation of **6** were used to assign values to the parameters in the PARM step of AMBER. Force constants were given high values to ensure that the tetrahedral geometry was preserved during the minimization process. Dihedral angles associated with the tetrahedral center were varied. As previously, we minimized at three values of dielectric constant; r, 3.0, and 30.0. Figure 5 illustrates the minimized tetrahedral intermediates derived from conformers LC2 and DT2. Numerical results for all of the conformers (at dielectric r) are listed in Table V.

Surfactant Mediated Reactions. To mimic the environment of a micelle, a new residue, a decyltrimethylammonium ion, was built,

(25) (a) Davidon, W. C. *Comput. J.* **1968**, *10*, 406. Fletcher, R. *Ibid.* **1965**, *8*, 33. (b) Fletcher, R.; Powell, M. J. D. *Ibid.* **1963**, *6*, 163. (c) Weiner, P. K. Ph.D. Thesis Dissertation, University of Texas, Austin, 1975.

(26) Available from Quantum Chemistry Program Exchange, Bloomington, Indiana.

(27) (a) Madura, J. D.; Jorgensen, W. L. *J. Am. Chem. Soc.* **1986**, *108*, 2517. (b) Burgi, H. B.; Lehn, J. M., Wipff, G. *Ibid.* **1974**, *96*, 1956.

(28) INSIGHT, a molecular graphics software package for the E&S PS-300, available from BIOSYM Inc., San Diego, CA.

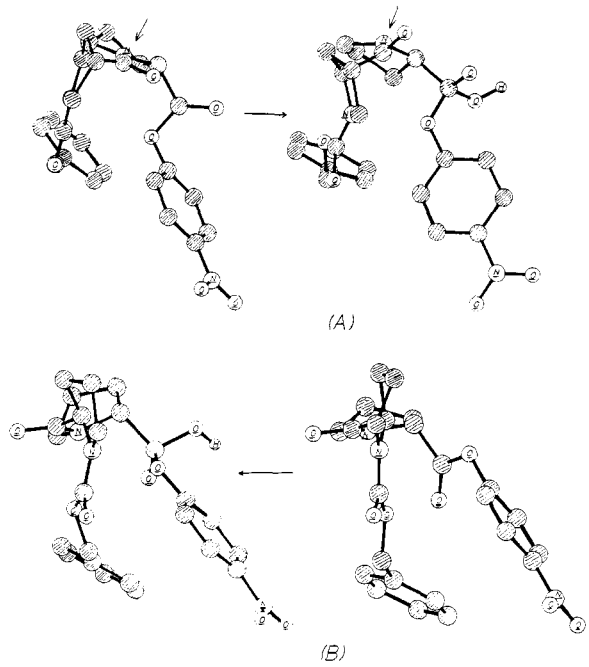

Figure 5. Minimum energy conformations of the ground-state molecules and the corresponding tetrahedral intermediates formed from the reaction of hydroxide ion with DL (A) and LL (B) Z-Pro-Pro-PNP. The arrows in the illustrations indicate the region in the vicinity of the Pro-Pro amide bond where a high degree of angle and torsional strain energy develops in the DL diastereomer when the tetrahedral intermediate is formed (see text). These illustrations represent the DL and LL conformers which had the lowest ΔE values (LC2 and DT2) in Table VII. The corresponding conformational parameters are in Table VIII. Heteroatoms are labeled. The shaded atoms represent carbons.

Table V. AMBER Energies for Tetrahedral Intermediates[a]

energy (kcal/mol)	LC1	LC2	LT3	DT1	DT2	DT3
total	14.13	10.80	22.56	21.57	21.01	25.04
bond	0.93	0.57	1.01	0.89	0.77	0.81
angle	21.35	16.05	19.77	16.96	16.17	18.81
dihedral	18.92	20.01	20.43	24.59	25.65	14.35
VDW	−12.28	−14.07	−7.49	−11.50	−13.08	−6.11
electric	−24.82	−21.18	−21.02	−19.01	−19.82	−12.56
1-4 VDW	11.48	10.95	10.59	11.85	12.46	11.78
1-4 EEL	−1.45	−1.53	−0.72	−2.21	−1.14	−2.04

[a] Calculation done with dielectric r (distance dependant).

assigned charges with MNDO, and minimized with AMBER, with the alkyl chain in the all-staggered conformation. This residue, with atomic charges, is shown in Figure 1. Ground-state complexes (assemblies) of this residue, a hydroxide ion, and a substrate molecule were created by using interactive graphics and several model building criteria. The substrate molecule was oriented with respect to the surfactant molecule so that electrostatic interactions between the ammonium nitrogen of the surfactant and carbonyl oxygens of the substrate would be maximized. At the same time, hydrophobic interactions between the molecules were maximized by orienting the substrate so that its aryl groups would be in close proximity to the alkyl chain of the surfactant. To minimize the effect of unpaired charges, the hydroxide ion was oriented at the van der Waal's distance from the ammonium ion on the side of the surfactant farthest away from the substrate. The resulting 1:1 substrate/surfactant complex was then energy minimized at dielectric constant values of r and 30.0.

A similar procedure was used to determine a starting point for the tetrahedral intermediate derived from the 1:1 complex, except that the hydroxide ion was now oriented at the van der Waal's distance from the carbonyl group of the reacting ester. Figure 6, A and B, illustrates the minimized tetrahedral intermediates derived from the 1:1 surfactant/DT3 or LC2 plus OH^- reactions. The depicted examples are calculated at a dielectric constant of

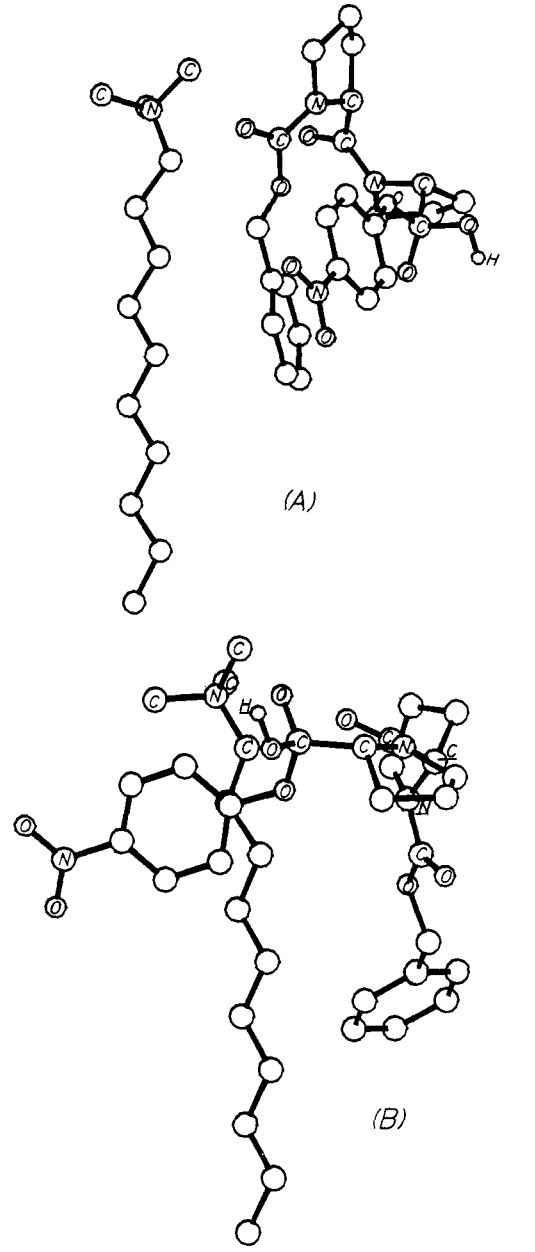

Figure 6. 1:1 surfactant/substrate tetrahedral assemblies for substrates LC2 (A) and DT3 (B), the two substrate molecules with the lowest ΔE values at a dielectric constant of 30 (see Table X). The tetrahedral coordinate reaction centers can be seen in the top center of illustration B and on the right in illustration A. The differences in orientation of the reaction centers with respect to the surfactant molecule are the result of applying the criteria for optimizing the electrostatic and van der Waals interactions (see text).

30 to mimic the Stern layer of a cationic surfactant (see below).

To model the reaction of a functionalized micellar surfactant with the substrates, we assumed that the ground state would be the 1:1 surfactant/substrate complex described previously and that the functional surfactant could be included as a constant perturbation on the ground state. We then took the minimized conformation of the tetrahedral intermediate of the 1:1 complex, removed the hydrogen from the OH group at the reaction center, and added a new residue (representing the functional surfactant) to the oxygen in place of the hydrogen. This residue [$-CH_2CH_2N(CH_3)_2C_9H_{19}$] appears in Figure 1.

The result is the tetrahedral intermediate from the attack of the oxyanion of a choline surfactant. The whole assembly was made to mimic a micellar structure by orienting its alkyl chain in the same direction as the decyltrimethylammonium surfactant chain. All assemblies thus formed were energy minimized as before. Figure 7 illustrates the 2:1 tetrahedral intermediate

Table VI. Conformational Parameters for Ground-State Substrates

dihedral angle[a]	LC1	LC2	LT3	DT1	DT2	DT3
ω_1	-3	-2	-1	5	2	-175
ϕ_2	-49	-55	-53	67	64	64
ψ_2	133	135	114	-110	-113	-117
ω_2	5	0	-176	170	170	170
ϕ_3	-62	-71	-56	-47	-45	-52
ψ_3	-64	107	115	115	-46	-48

[a] IUPAC-IUB recommended nomenclature (see ref 37). Angles in degrees.

complexes, derived from the DT3 and LC2 substrates.

Initially we planned to construct a tetrahedral intermediate corresponding to the attack of a thiocholinate surfactant that would better model the reactions of 16-S$^-$. However, MNDO calculations for the reactions of CH_3S^- (or HS^-) with methyl acetate failed to yield stationary points for tetrahedral geometries. Accordingly, the cholinate analogue of 16-S$^-$ had to be used in the modeling.

Results and Discussion of Calculational Studies

Initial Conformations. Conformational parameters for the backbone dihedral angles of the six selected low-energy conformations are shown in Table VI. For the LL substrates, these values are in general agreement with analytical results for oligopeptides[29] as well as the results of conformational energy mapping of proline dipeptides.[30]

Examination of Table III shows that for the LL substrate, the lowest energy conformation, LC1, has a cis arrangement for the amide bond between the proline rings. The energy difference between the lowest energy cis and trans conformers is 0.73 kcal/mol, which amounts to a 3.5:1 cis/trans ratio at 25 °C. Previous investigations of various substituted Pro-Pro oligomers, in both solution and the solid state, seem to indicate that a trans preference is more common.[29] There are exceptions, however, and in any case, the difference in energy between the cis and trans isomers is small enough so that both conformers should coexist in solution at room temperature. Also, intramolecular van der Waals interactions are stronger for the cis conformer, suggesting that the addition of the *p*-nitrophenyl group to the C terminus may be the stabilizing factor.

For the DL Pro-Pro dipeptides cis amide bonds are sometimes energetically preferred.[29] However, our calculations indicate that the 3 lowest energy conformations of DL-**4** contain trans Pro-Pro peptide linkages; a "cis" conformer is the fourth lowest energy conformation. Again, van der Waals interactions are strong and may be the major factor influencing this conformational preference. In our previous analysis of the experimental diastereoselectivities (above),[3,8] we began with hand-held molecular models fixed in trans AA-Pro peptide conformations. The present results, suggesting that cis conformers play a major role in the chemistry of the LL substrate, necessitate changes in our mechanistic analysis of micellar diastereoselectivity; see below.

Rationale for Construction of the Tetrahedral Intermediate. It is generally accepted that esterolysis reactions in aqueous media take place through the formation sp^3-hybridized tetrahedral intermediates.[31,32] In this scheme, it is assumed that the reaction proceeds from the ground-state nucleophile and substrate, over an activation barrier, to a metastable tetrahedral intermediate. The intermediate can revert back to the starting materials or proceed over a second activation barrier, where the leaving group is expelled, and the geometry around the reacting carbon atom returns to planar sp^2. The rate-determining step for the overall

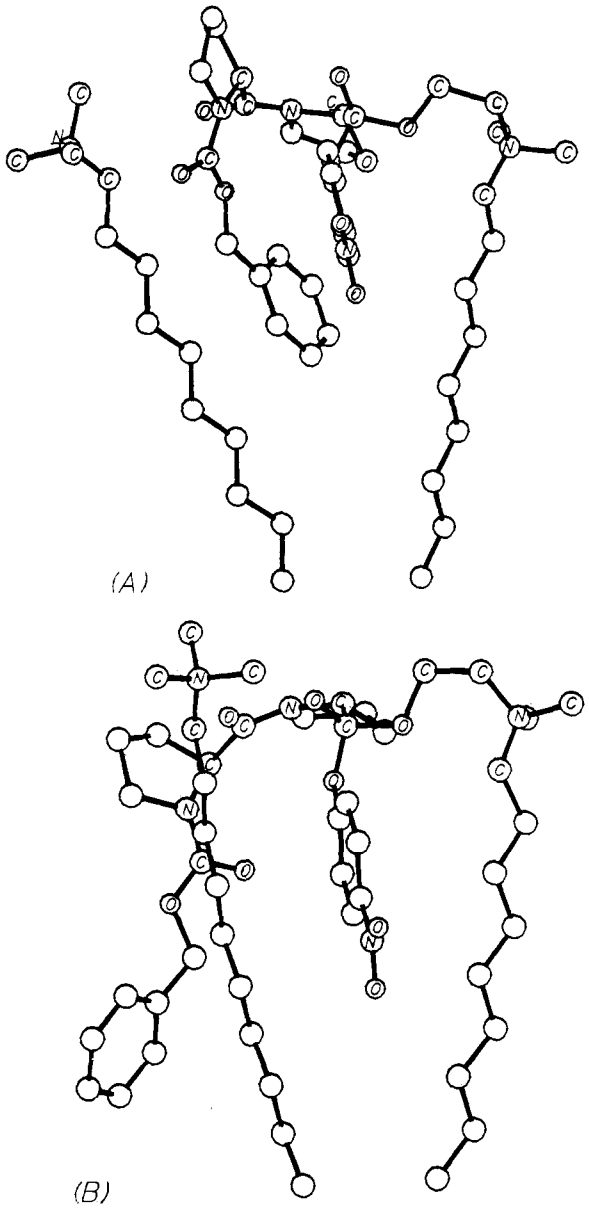

Figure 7. 2:1 tetrahedral intermediate assemblies resulting from nucleophilic attack of a choline oxyanion surfactant. The substrate molecules are conformers LC2 (A) and DT3 (B). These conformers had the lowest ΔE values when the energy was minimized at a dielectric constant of 30 (see Table XI).

process is dependent upon the differences in activation free energy between the two steps as measured relative to the tetrahedral complex. In the reactions studied here, the leaving group is a highly stable *p*-nitrophenoxide anion. This favors the breakdown of the intermediate to products. Furthermore, the electron-withdrawing nitro group promotes bond cleavage in the second step of the esterolysis, by lowering the activation barrier for this step.[32] Thus, we assume that the rate-determining step in the reactions discussed here is the first step, attack of the nucleophile to form the tetrahedral complex.

There have been several theoretical studies of attack by hydroxide ion or other nucleophiles on acids, esters, and aldehydes leading to tetrahedral intermediates.[33] These studies suggest that the energetics of the reactions are greatly influenced by the reaction medium. In the gas phase, the reaction proceeds exothermically. On the other hand, ab initio calculations, coupled with Monte Carlo[27a] or molecular mechanics[11] simulations, in agreement with experiment, predict the activation barrier to in-

(29) Benedetti, E.; Bavoso, A.; di Blasio, B.; Pavone, V.; Pedone, C.; Toniolo, C.; Bonora, G. M. *Biopolymers* **1983**, *22*, 305.
(30) Balaram, H.; Prasad, B. V. V.; Balaram, P. *J. Am. Chem. Soc.* **1983**, *105*, 4065.
(31) (a) Bender, M. L. *J. Am. Chem. Soc.* **1951**, *73*, 1626. (b) Bender, M. L. *Chem. Rev.* **1960**, *60*, 53. (c) Bender, M. L. *J. Am. Chem. Soc.* **1967**, *89*, 1211.
(32) Jencks, W. P. *Catalysis in Chemistry and Enzymology*; McGraw Hill: New York, 1969; Chapter 10.
(33) Oie, T.; Loew, G. H.; Burt, S. K.; MacElroy, R. D. *J. Comput. Chem.* **1983**, *4*, 449. See also ref 11 and 27.

Table VII. $\Delta E_{tet\text{-}gs}$ for Tetrahedral Intermediate Formation in Aqueous Solution[a]

energy (kcal/mol)	LC1	LC2	LT3	DT1	DT2	DT3
total	2.121	−2.479	9.824	10.389	10.296	14.791
bond	0.38	0.06	0.50	0.35	0.24	0.31
angle	5.64	0.89	4.62	1.94	1.19	4.29
dihedral	5.66	5.10	6.50	10.45	11.96	0.17
VDW	1.25	0.07	2.28	−0.45	0.49	7.00
electric	−7.25	−4.38	0.44	3.52	0.36	7.88
1-4 VDW	0.84	0.39	−0.16	0.81	1.48	0.64
1-4 EEL	−4.41	−4.71	−4.35	−6.22	−4.42	−5.21

[a] Calculation done with dielectric r (distance dependant).

termediate formation to be 20–28 kcal/mol. The high activation barrier in solution has been attributed to required desolvation of the reactant partners necessary for them to come close enough for the reaction to proceed.[34] If, in the esterolysis of Z-Pro-Pro-PNP, solvation effects on the diastereomeric systems are roughly equal, then the differences in reactivity may be traceable to differential conformational strain energy during intermediate formation.

Although we have modeled the intermediate and not the transition state leading to the intermediate, the tetrahedral complex, because it is fully sp^3 hybridized, represents the maximum distortion of the reaction center (carbonyl carbon) from planarity (the ground-state geometry) and therefore should sensitively reflect the conformational energy changes leading to the reactivity differences. The transition-state geometry is intermediate between planar and tetrahedral, and as a result the ΔE values derived from the tetrahedral geometry will overestimate the energy differences that generate the rate differences. Also, because we constrain the tetrahedral geometry around the reaction center, we probably overestimate the energy differences between the intermediate and the ground state. We assume, however, that the overestimations are comparable for reactions of LL and DL substrates, so that comparisons of ΔE values (see below) are valid.

Aqueous Reaction. Assuming that the hydroxide ion is a uniform perturbation on the energies of the ground-state systems, we can subtract the E values of Table III from those of Table V to obtain ΔE values related to the activation energies for the reactions taking place in solution. Table VII presents these results. These calculations predict that the LL diastereomer should react more rapidly than the DL diastereomer with hydroxide ion in solution. This is in agreement with experiment as shown above in Table I. As we have stated previously, the ΔE values are overestimated, due to the nature of the modeling process. We can see this in Table VII, from which we would expect the LL substrate to react with OH^- *much* more rapidly than the DL substrate because $\Delta\Delta E$ (LC2 vs. DT2) is ~12.8 kcal/mol. In reality, the rate constant difference of ~2 reflects a free energy of activation difference <1 kcal/mol. Of course the calculated ΔE values ignore entropy changes. These are clearly significant and may play a major role in real $\Delta G^{\ddagger}$ values.

The principal origin of the larger ΔE for the DL diastereomer is not the same for each conformer studied. The conformers DT1 and DT2 have higher ΔE values in comparison to the LL conformers largely due to increased dihedral strain energy (illustrated in Figure 5), whereas the DT3 conformer has larger van der Waals and repulsive electrostatic energy terms.

According to the Curtin–Hammett principle,[35] when a reaction is slow compared to the rate of substrate conformational equilibration, the product composition depends solely on the relative activation barriers between competing product-forming processes. For glycine-proline dipeptides, the activation energy for cis–trans isomerism about the amide bond has been found to be 20 kcal/mol.[36] This corresponds to a rate constant of 0.02 s^{-1} at 25 °C, 1–2 orders of magnitude greater than the pseudo-first-order rate constants for alkaline hydrolysis (cf. Table I). Therefore, the identity of the predominant ground-state conformer in solution is irrelevant; the reaction takes place through the conformation that affords the lowest ΔE.

Table VIII. Conformational Parameters for Tetrahedral Intermediates in Aqueous Solution[a]

dihedral angle[b]	LC1	LC2	LT3	DT1	DT2	DT3
ω_1	−23	−18	−19	−21	−23	165
ϕ_2	−5	−4	−4	115	115	16
ψ_2	140	99	89	−109	−116	−133
ω_2	−45	23	135	127	126	170
ϕ_3	−3	−116	−4	−4	−4	−2
ψ_3	−63	69	70	−54	−66	−65

[a] Calculation done with a distance dependent dielectric (r). See Figure 5 and Table V for energies. [b] IUPAC-IUB recommended nomenclature (see ref 37).

Table IX. $\Delta E_{tet\text{-}gs}$ Values for Intermediate Formation in 1:1 Complexes[a]

energy (kcal/mol)	LC1	LC2	LT3	DT1	DT2	DT3
total	18.765	16.630	23.883	32.724	20.796	24.305
bond	0.34	0.08	0.44	0.40	0.27	0.36
angle	5.59	1.10	4.11	1.76	0.51	2.63
dihedral	5.92	5.47	6.78	10.66	11.29	3.79
VDW	0.61	−2.00	3.21	−0.63	3.31	5.66
electric	11.86	16.39	13.54	26.05	8.45	16.34
1-4 VDW	0.06	0.18	0.41	0.53	1.44	0.89
1-4 EEL	−4.40	−4.58	−3.72	−6.05	−4.47	−5.58

[a] Calculation done with distance dependent dielectric (r).

Table X. $\Delta E_{tet\text{-}gs}$ Values for Intermediate Formation in 1:1 Complexes[a]

energy (kcal/mol)	LC1	LC2	LT3	DT1	DT2	DT3
total	12.896	7.934	12.617	14.767	15.014	12.836
bond	0.436	0.129	0.486	0.487	0.310	0.272
angle	6.571	1.699	5.954	2.718	1.473	2.800
dihedral	4.041	4.101	1.92	5.40	6.432	1.025
VDW	1.247	0.948	5.529	4.259	5.701	8.043
electric	0.622	0.940	−0.306	1.485	0.463	0.566
1-4 VDW	0.639	0.491	−0.588	0.865	0.982	0.505
1-4 EEL	−0.360	−0.051	−0.381	−0.437	−0.346	−0.376

[a] Calculation done with dielectric constant 30.0.

To examine the origin of the enhanced diastereoselectivity in aqueous alkaline hydrolysis, we should therefore compare the ΔE values for conformers LC2 and DT2 or DT1 (Table VII). Here, we can see that the major contributions stem from increased dihedral strain energy in the DL cases (a change in dielectric constant to $\epsilon = 30$ changes our choice of conformers but not the conclusion). An analysis of the separate contributions to the dihedral energies shows that distortions of the amide bond between the proline rings, and the dihedral angles associated with it, make the major contributions to the strain energy. The indications are that the greater reactivity of the LL substrate derives from the fact that the most reactive conformation of the LL diastereomer suffers less distortion of its peptide and associated dihedral angles upon conversion to the tetrahedral intermediate, and at lower energy cost, than does the corresponding DL diastereomer. Table VIII lists the conformational parameters for the tetrahedral intermediates. Comparison of Tables VIII and VI shows that $\Delta\omega_2$ (the peptide dihedral) for LC2 is 23°, whereas for DT2 it is 44°. Similarly, other dihedral angles, such as O-C-C^{α}-N, are more distorted for the DL substrate. Figure 5 illustrates these effects with molecular graphics.

Micellar Reaction. Applying the same procedure and reasoning to the reactions involving a single nonfunctionalized surfactant

(34) Houk, K. N.; Padden-Row, M. N.; Rondan, N. G.; Wu, Y. D.; Brown, F. K.; Spellmeyer, D. C.; Metz, J. T.; Li, Y.; Loncharich, R. J. *Science* **1986**, *231*, 1108.
(35) For a review see: Seeman, J. I. *Chem. Rev.* **1983**, *83*, 83.
(36) Cheng, H. N.; Bovey, F. A. *Biopolymers* **1977**, *16*, 1465.
(37) *Biochemistry* **1970**, *9*, 3471.

Table XI. $\Delta E_{tet\text{-}gs}$ Values for Intermediate Formation in 2:1 Complexes[a]

energy (kcal/mol)	LC1	LC2	LT3	DT1	DT2	DT3
total	10.134	9.513	9.748	33.914	14.768	12.317
bond	0.693	0.742	0.728	0.689	0.603	0.718
angle	9.266	9.736	6.790	10.923	3.020	4.211
dihedral	3.654	1.625	1.667	15.069	11.553	6.507
VDW	−6.665	−6.221	−2.055	5.560	−3.980	−2.030
electric	−0.565	−0.491	−1.780	0.047	−0.914	
1-4 VDW	3.123	3.521	4.331	3.720	3.789	3.731
1-4 EEL	0.627	0.924	−0.024	−0.095	−0.024	−0.014

[a] Calculation done with dielectric constant 30.0.

Table XII. Effect of Dielectric on ΔE of Reactions in Aqueous Solution[a]

dielectric	LC1	LC2	LT3	DT1	DT2	DT3
r	4.60	0.00	12.303	12.868	12.775	12.720
3.0	8.443	3.571	8.198	12.437	12.502	14.852
30	15.208	8.327	8.378	13.681	14.872	14.529

[a] All values normalized to LC2 = −2.479; see Table VII. Values are ΔE (kcal/mol) for tetrahedral intermediate formation from the indicated conformer at each dielectric.

molecule (1:1 assembly), we reach parallel conclusions. The rates of alkaline hydrolysis in the presence of nonfunctional CTACl micelles are probably within an order of magnitude of the rate of conformer cis-trans isomerization, so that Curtin-Hammett conditions may still apply. If we choose a dielectric value of *r* (distance dependent), then the two diastereomers we compare are again LC2 and DT2 (see Table IX). Here again, the significant differences in reactivity can be attributed to dihedral distortion around the Pro-Pro peptide bond and also to a better van der Waals interaction energy for the LL substrate. On the other hand, if we use a dielectric constant of 30, we must compare DT3 and LC2 (see Table X) where these 2 diastereomers are calculated to have the lowest ΔE. In this comparison, the rate differences would be mainly attributed to the greater van der Waals repulsion energy in DT3.

Both the LC2 vs. DT2 comparison with a dielectric of *r* and the LC2 vs. DT3 comparison with a dielectric of 30 lead to similar $\Delta\Delta E$ values (ca. 4 or 5 kcal/mol) in favor of more rapid reaction from the LL substrate. This is in agreement with experiment (Table I). Experimentally k^{LL}/k^{DL} is small (only ~2) in CTACl micelles, so that, as before, the advantage of the LL substrate is overestimated by the calculations.

Functionalized Micellar Reaction. For reactions taking place by means of nucleophilic attack by functionalized micellar surfactants such as 16-SH or 16-IO (Table II), the pseudo-first-order rate constants are all greater than the likely rate constants for cis-trans interconversion of the peptide bonds. Accordingly, interconversion of ground-state conformation becomes an important factor. We must now consider all low-energy conformations and compare all of the ΔE values. These are shown in Table XI. For the LL conformers we see that the ΔE values differ by no more than ~0.6 kcal/mol and are at least 2 kcal/mol lower than ΔE for the lowest energy DL substrate conformer. This indicates that, with reference to the conformations studied here, the LL diastereomer should react faster than the DL diastereomer. This is in agreement with experiment; see Table II. However, the calculated ΔE and $\Delta\Delta E$ values (Table XI) fail to reflect the enhancement in k_ψ^{LL}/k_ψ^{DL} observed when the reaction system changes from nonfunctional CTACl micelles and a hydroxide nucleophile (Table I) to functional thiocholinate or iodosobenzoate surfactant micelles (Table II). Given the many assumptions in our calculational approach, this is not surprising. It is perhaps sufficient success at this level to have modeled the *sense* of the diastereoselectivity in each of the three reaction systems (buffer, nonfunctional, and functional surfactant).

Choice of Dielectric Constant. In modeling the ground-state conformers and the reactions of hydroxide ion with these conformers, the choice of the dielectric damping factor does not affect the conclusions. In Table XII we show the effect of varying the dielectric on the ΔE of the reactions in aqueous solution (cf. Table VII, above). We performed calculations at $\epsilon = r$, 3.0, and 30.0. Except for one case at $\epsilon = 30.0$, all of the ΔE values for reactions of the LL substrate are below those for the DL substrate.

Table XIII. Effect of Dielectric on ΔE of Reactions of 1:1 Surfactant/Substrate Systems[a]

dielectric	LC1	LC2	LT3	DT1	DT2	DT3
r	10.831	8.696	15.945	25.33	12.862	16.371
30	4.962	0.0	4.683	6.833	7.08	4.902

[a] All values normalized to LC2 = 7.934; see Table X. Values are ΔE (kcal/mol) for tetrahedral intermediate formation from the indicated conformer at each dielectric.

Table XIV. Effect of Dielectric on ΔE of Reactions of 2:1 Surfactant/Substrate Systems[a]

dielectric	LC1	LC2	LT3	DT1	DT2	DT3
r	3.181	2.618	5.684	19.528	3.046	2.082
30	4.962	0.0	0.235	24.401	5.165	2.804

[a] All values are normalized to LC2 = 9.513; cf. Table XI. Values are ΔE (kcal/mol) for tetrahedral intermediate formation from the indicated conformer at each dielectric.

For reactions in water, however, we believe that the most appropriate dielectric is the distance dependent $\epsilon = r$. This conclusion is based upon a previous theoretical analysis indicating that, in solution, dielectric damping tends to increase in a roughly linear fashion.[38] Also, previously successful molecular mechanics[39] and dynamics[40] calculations, as well as qualitative agreement with experimental results, support the choice of $\epsilon = r$.

A referee has suggested, however, that these reasons are insufficient to favor the use of $\epsilon = r$ over 80 for the reaction in water. At $\epsilon = 80$, practically the same differential energies would be expected as at $\epsilon = 30$, so this would have the effect of restricting comparisons to $\epsilon = 30$. Nevertheless, the conclusions reached above would not change; in water, where Curtin-Hammett conditions apply, the cleavage reactions at $\epsilon = 30$ would mainly occur from LL conformers LC2 or LT3 and probably from all 3 of the ΔE-comparable DL conformers (see Table XII). Again (as with $\epsilon = r$), we would predict faster reaction of the LL substrate.

In modeling the micellar environment, we have no precedent to guide us in the choice of a dielectric constant. The micellar environment is discontinuous, and microscopically anisotropic in physical parameters such as dielectric constant. For these cases, we performed the calculations at dielectric values of $\epsilon = 30$ and *r*. Comparisons of results for the 1:1 and the 2:1 surfactant/substrate systems appear in Tables XIII and XIV, respectively. Our preferred choice of $\epsilon = 30$ is based on spectroscopic determinations of the effective dielectric at the Stern layer of cationic micelles.[41] For the 2:1 system, better qualitative agreement with experiment is obtained when we use $\epsilon = 30$.

Conclusions: Comparison of Experiments and Calculations

Cleavages of diastereomeric Z-Pro-Pro-PNP dipeptide esters **4** are LL diastereoselective when the nucleophile is hydroxide ion in bulk aqueous solution or in CTACl micellar solution, and also when the esterolysis occurs in thiolate or iodosobenzoate functional micellar media. There is a modest innate preference for LL diastereoselectivity that attends these intermolcular esterolyses, that also extends to the Z-Trp-Pro-PNP diastereomeric substrates, and that is significantly enhanced in functional micellar systems.

Molecular mechanics calculations of ground-state substrates and the putative tetrahedral intermediates derived from the attacks of hydroxide ion or surfactant cholinate ion on the substrates lead

(38) Warshel, A. *J. Phys. Chem.* **1979**, *83*, 1640.
(39) Blaney, J. M.; Weiner, P. K.; Dearing, A.; Kollman, P. A.; Jorgensen, E. C.; Oatley, S. J.; Burridge, J. M.; Blake, C. C. F. *J. Am. Chem. Soc.* **1982**, *104*, 6424.
(40) McCammon, J. A.; Wolynes, P. G.; Karplus, M. *Biochemistry* **1979**, *18*, 927.
(41) Fendler, J. H. *Membrane Mimetic Chemistry*; Wiley: New York, 1982; pp 19 and 20.

to ΔE values that are consistent with the observed LL diastereoselectivities. The calculations suggest that a principal origin of the stereoselectivity is the dihedral angle (torsional) strain of the peptide and associated bonds that attends trigonal to tetrahedral ester carbonyl rehybridization during the attack of the nucleophile. This strain is greater with the DL substrate which, accordingly, reacts more slowly.

The calculations do predict the LL diastereoselectivity observed in the hydroxide ion cleavages of the Pro-Pro substrates (although they greatly overestimate the kinetic preference), and they continue to predict LL diastereoselectivity, as is observed, in the presence of nonfunctional and functional surfactants. However, they fail to mirror the enhancement in LL preference seen in the latter case.

The calculations have a major effect on our view of micellar diastereoselectivity. Originally, we assumed that *both* LL and DL substrates reacted from trans conformations[29] and examined their interactions with surfactant molecules using 1:1 assemblies of hand-held models.[8] Subsequently, we found that 1:1 substrate/surfactant reactions cannot account for the diastereoselectivity,[9] and *now* we find, at least for the Pro-Pro substrates, that the LL isomer may well react (at least in part) from cis peptide conformations. The importance of the latter point can be appreciated on inspection of Figures 6A/6B and 7A/7B.

The DT3 tetrahedral intermediates (B parts of the figures), reacting from trans peptide conformers, display the "hydrophobic clefts" previously discerned in the hand-held models,[8] and the surfactant chain appears to bind therein. However, LC2 (A parts of the figures), reacting from a cis conformer that lacks the "extended" (trans) peptide link, cannot similarly "wrap around" the surfactant chain. Instead, it adopts a compressed, almost globular shape, where internal hydrophobic interactions can be maximized. This structure will fit *between* the surfactant molecules in a micelle (cf. Figure 7A) and should be sensitive to structural transitions within the aggregate, e.g., sphere to rod. It is known that low concentrations of LL-Trp-Pro-PNP induce just such a transition in 16-S^- micelles and that the transition is directly coupled to the onset of kinetic diastereoselectivity.[9b] The "nutcracker" arrangement of LC2-OH, depicted in Figure 7A, appears well-suited for the transduction of changes in surfactant packing, which attend an aggregate transition, into energetic effects at the reaction center.

On the other hand, the extended conformer of DT3-OH (Figure 7B) may resist surfactant close packing. DL-Trp-Pro-PNP does not induce a transition in 16-S^- micelles, at least not at surfactant concentrations where the LL substrate is effective.[9b] The differences in LL and DL conformations, shown in Figures 6A/6B and 7A/7B, may therefore be directly related to the packing of surfactant monomers around these isomeric substrates, to the structures of the aggregates that contain the substrates, and hence to the abilities of the aggregates to elicit kinetic diastereoselectivity.

It remains to be seen whether calculational studies of the Trp-Pro substrates will also show the cis-LL/trans-DL conformational preferences found for the Pro-Pro substrates and, experimentally, whether the LL-Pro-Pro (but not the DL-Pro-Pro) substrates can induce sphere-to-rod transitions in 16-S^- micelles. Both of these parallels should hold if the foregoing speculative analysis of the origins of micellar diastereoselectivity has any merit.

Experimental Section[42]

Surfactants. CTACl (**1**) was obtained from Eastman and was recrystallized several times from anhydrous ethanol/ether. 16-SH (**2**) and 16-IO (**3**) were available from other studies; their preparation, purification, and properties have been fully described.[15,16]

Substrates. *N*-Carbobenzyloxy-L-prolyl-L-proline *p*-Nitrophenyl Ester, Z-L-Pro-L-Pro-PNP (LL-4). *p*-Nitrophenyl-*N*-carbobenzyloxy-L-proline (Sigma) was deprotected in dry HBr-saturated acetic acid for 2 h at room temperature.[43] This compound was dried, after washing with dry ether, and used in coupling reactions without further purification.

N-Carbobenzyloxy-L-proline (Sigma) (748 mg, 3.0 mmol) was dissolved in 30 mL of dry methylene chloride. The initial suspension became a clear solution after the addition of 0.415 mL (3.2 mmol) of triethylamine at −10 °C. Then, 326 mg (3.0 mmol) of ethyl chloroformate was added, and the solution was stirred for 20 min under nitrogen. After 953 mg (3.0 mmol) of *p*-nitrophenyl-L-prolinate hydrobromide was added, the reaction was started by the addition of 0.415 mL (3.2 mmol) of triethylamine to the reaction mixture over 10 min. The final yellow solution was stirred in the cold (−5 to 0 °C) for 2 h and then for an additional 3 h at room temperature. The organic solution was washed with water (2 × 15 mL), 1 N HCl (2 × 15 mL), additional water (1 × 15 mL) and then dried over $MgSO_4$. A slightly yellow viscous oil was obtained after the solvent was evaporated. The crude product was purified by column chromatography (250:125:1 ethyl acetate/*n*-hexane/acetic acid eluent over 230–400 mesh silica gel (Sigma)). The final product was obtained in 62% yield as a white solid after evaporating the solvent to dryness at room temperature: mp <15 °C, TLC with ethyl acetate/*n*-hexane/acetic acid (250:125:1), or with dichloromethane/methanol (20:1) on silica gel gave single spots, R_f 0.22 or 0.47, respectively; IR ($CHCl_3$) 1760 (s), 1696 (s), 1653 (s), 1607 (w), 1592 (w) cm^{-1}; NMR (80 MHz, δ, $CDCl_3$), 8.25 (d, J = 8.8 Hz, 2 H, PNP), 7.34 + 7.27 (m + s at 7.34, 7 H, 5 H from OCH_2Ph + 2 H from PNP), 5.11 (m, AB, 2 H, OCH_2Ph), 4.48 (m, 2 H, H_αPro), 3.56 (m, 4 H, H_δPro), 2.04 (m, 8 H, H_βPro + H_γPro). The specific rotation was $[\alpha]^{23}D$ −126.9° (*c* 1.0, methanol).

Anal. Calcd for $C_{24}H_{25}N_3O_7$: C, 61.64; H, 5.39; N, 8.99. Found: C, 61.11; H, 5.32; N, 8.84. The marginally low C analysis may be due to traces of water.

***N*-Carbobenzyloxy-D-prolyl-L-proline *p*-Nitrophenyl Ester, Z-D-Pro-L-Pro-PNP (DL-4).** *N*-Carbobenzyloxy-D-proline (Sigma) was coupled to *p*-nitrophenyl L-prolinate, using the same procedure employed for the LL diastereomer (see above). The final product was obtained in 48% yield as a white solid; mp < 15 °C. TLC with ethyl acetate/*n*-hexane/acetic acid (250:125:1) or with dichloromethane/methanol (20:1) on silica gel gave single spots, R_f 0.14 or 0.44, respectively. The specific rotation was $[\alpha]^{23}D$ −35.7° (*c* 1.0, methanol); IR ($CHCl_3$) 1758 (s), 1693 (s), 1650 (s), 1603 (w), 1588 (w) cm^{-1}; NMR (80 MHz, δ, $CDCl_3$), 8.18 (m, 2 H, PNP), 7.30 (m, 7 H, 5 H from OCH_2Ph + 2 H from PNP), 5.08 (m, AB, 2 H, OCH_2Ph), 4.57 (m, 2 H, H_αPro), 3.60 (m, 4 H, H_δPro), 2.08 (m, 8 H, H_βPro + H_γPro).[44]

Anal. Calcd for $C_{24}H_{25}N_3O_7$: C, 61.64; H, 5.39; N, 8.99. Found: C, 61.66; H, 5.41; N, 9.06.

***N*-Carbobenzyloxy-(L or D)-tryptophanyl-L-proline *p*-Nitrophenyl Ester, Z-D or L-Trp-L-Pro-PNP (5).** These diastereomeric substrates were available from another study; their preparation, purification, and characterization have been fully described.[9b]

Kinetic Studies. Kinetic techniques and results are described above (Results), and in Tables I and II. For additional details, see Ref. 16.

Acknowledgment. We are grateful to the U.S. Army Research Office and the donors of the Petroleum Research Fund, administered by the American Chemical Society, for financial support. We thank S. L. Gallion for helpful discussions and for the use of his torsional mapping program. We acknowledge with pleasure instrument support from the National Science Foundation for the purchase of the graphics and computer systems.

Supplementary Material Available: Tables of additional parameters for AMBER, and AMBER energies for initial conformations at various dielectric constants (3 pages). Ordering information is given on any current masthead page.

(42) Melting points are uncorrected. IR spectra were recorded on a Perkin-Elmer Model 727B instrument. NMR spectra were recorded at 80 MHz on a Varian FT-80 spectrometer. Optical rotations were measured on a Perkin-Elmer Model 141 digital polarimeter. Microanalyses were carried out by Robertson Laboratory, Florham Park, NJ.

(43) Ben-Ishai, D.; Berger, A. *J. Org. Chem.* **1952**, *17*, 1564.

(44) The enantiomer of DL-**4** (LD-**4**) was prepared by an identical procedure from *Z*-L-Pro and D-Pro-PNP. The NMR spectrum of LD-4 was identical with that of DL-**4** and significantly different from that of LL-**4**.